A sub-domain meshless method based on combination of weak and strong forms

Yong-Ming Guo*, Tatuya Hamada, Genki Yagawa, and Shunpei Kamitani

***Abstract*—**A sub-domain method is often used in computational mechanics. The conforming sub-domains are often used, while the nonconforming sub-domains could be employed if needed. In the latter cases, the integrations of the sub-domains may be performed easily by choosing a simple configuration. Then, the meshless method with nonconforming sub-domains is considered one of the reasonable choices. We have proposed the sub-domain meshless method (SDMM). In this work, a nonlinear problem is analyzed by using the proposed SDMM. The numerical solutions show that the relative errors by using the SDMM are small and that the proposed method possesses a good convergence.

***Keywords*—**Sub-domain method, meshless method, weak and strong forms, nonlinear problem.

I. Introduction

A lot of meshless methods have been published. In the meshless techniques, complicated non-polynomial interpolation functions are often used, which renders the integration of the weak form rather difficult. Failure to perform the integration accurately results in loss of accuracy. Chen et al. have proposed some integration methods called the stabilized conforming nodal integration (SCNI) [1] and the variation consistency (VC) integration [2] to recover the Galerkin orthogonality in the meshless methods, showing the applicability of the Galerkin meshless method using the SCNI or the VC to some problems of the computational mechanics. In the former, the conforming (not separated nor overlapped) integration is used, which is troublesome for irregular nodal distribution and is known to require much computer time. Then, an accurate and easy integration technique is desired for the meshless methods of the weak form.

On the other hand, a lot of the methods with the collocation in the strong form have been proposed in the literature. Meanwhile, the methods with the collocation in the strong form have no issues of the integration scheme, since the integrations are not needed. It has been known, however, that the collocation methods (CM) have issues of violation of the positivity conditions that the violation of the positivity conditions may result in a large error in the numerical solution [3]-[5]. The positivity conditions are some inequalities on the shape function and its second-order derivatives. To improve the robustness of the CM, Jin et al. [5] have proposed techniques, based on modification of weighting functions, to ensure satisfaction of positivity conditions when using a scattered set of points. For boundary points, however, the positivity conditions cannot be satisfied, obviously. To overcome the demerit of CM, the over-range collocation method (ORCM) has been proposed [6]. In ORCM, some over-range collocation points are introduced which are located outside of the body to be analyzed. Some boundary value problems including the Poisson's equation, the linear elastic cantilever beam [6], and the nonlinear partial differential equations [7] have been analyzed by using the ORCM, showing that the method works well for these boundary value problems. Also, it has been shown that the positivity conditions of the boundary points in the method are satisfied by the employment of the over-range points [8].

In order to get an accurate and easy integration technique for the meshless methods of the weak form, the present authors have proposed the sub-domain meshless method (SDMM) [9]. As is well known, the sub-domain method, in which the problems are solved by dividing a domain to be solved into multiple sub-domains, is popular in computational mechanics. The conforming sub-domains, where the sub-domains are not separated nor overlapped each other, are usually used. However, since the SDMM can employ both the conforming and the nonconforming sub-domains, it is possible to use nonconforming sub-domains of simple configuration (for example, square or hexahedron ones), making the integration at the sub-domain very simple. The nonconforming (separated or overlapped) sub-domains for integration with square configuration are shown in Fig. 1. However, on the boundary of the analysis domain with a complicated shape, it is difficult to select a sub-domain of simple configuration. To overcome this problem, we apply the collocation approach to the nodes on the boundary, then no integration is needed for the nodes on the boundary. In addition, in order to satisfy the positivity conditions for the boundary nodes, the over-range points [6] are added. The mixed boundary value problems about the Poisson equation and the Helmholtz equation have been analyzed by

Yong-Ming Guo, Tatuya Hamada, and Shunpei Kamitani are with University Kagoshima, Kagoshima City, Japan (corresponding author to provide phone: 099-285-8258; fax: 099-285-8258; e-mail: guoy@mech.kagoshima-u.ac.jp).

Genki Yagawa is the emeritus professor of the University of Tokyo, Tokyo, Japan.

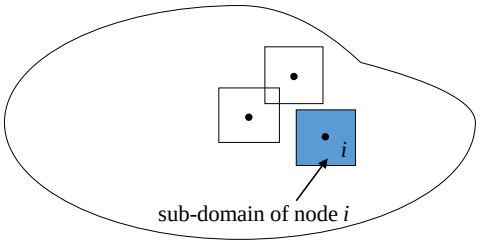

Fig. 1 Nonconforming (separated or overlapped) and simple-shaped sub-domains employed at each node for integration.

using the SDMM [9].

As is well known, nonlinear problems are difficult problems of the computational mechanics. In this paper, the boundary value problems of the above-mentioned challenge issues are analyzed by using the SDMM, which are compared with the exact solutions and the solutions of the CM. The CM used in this study is the classical collocation method, in which no over-range point is used.

II. Formulation of the SDMM

Let us consider a scalar boundary value problem defined as follows:

$$D(u) = b\,, \quad over\ \Omega\,. \tag{1}$$

with boundary conditions

$$u - u_c = 0\,, \quad on\ \Gamma_u\,. \tag{2}$$

$$T(u) = t\,, \quad on\ \Gamma_t\,. \tag{3}$$

to be satisfied in a domain Ω with boundary $\Gamma = \Gamma_t \cup \Gamma_u$, where D and T are appropriate differential operators, u is the problem unknown function, b and t are external forces or sources acting over Ω and along Γ_t, respectively, u_c is the assigned value of u over Γ_u.

Here, let us assume that the ith sub-domain for integration is Ω_i. On the other hand, we assume a sub-domain for interpolation Ω_x, which is the neighborhood of a point x_1 in the domain. The distinction of the two kinds of sub-domain (Ω_x and Ω_i) is shown in Fig. 2. Then, we assume an approximation u^h of u over Ω_x defined by:

$$u^h(\boldsymbol{x}) = \boldsymbol{N}(\boldsymbol{x})\hat{\boldsymbol{u}}\,. \tag{4}$$

where $\hat{\boldsymbol{u}}$ may be defined as

$$\hat{\boldsymbol{u}} = [\hat{u}_1 \quad \hat{u}_2 \quad \cdots \quad \hat{u}_n]^T. \tag{5}$$

and n is the number of nodes randomly located in the sub-domain Ω_x. $\boldsymbol{N}(\boldsymbol{x})$ is the shape function. Substituting (4) into (1)-(3) at each sub-domain Ω_x, the following residuals R_1, R_2 and R_3 are obtained:

$$D(\boldsymbol{N}(\boldsymbol{x})\hat{\boldsymbol{u}}) - b = R_1, \quad over\ \Omega\,. \tag{6}$$

$$\boldsymbol{N}(\boldsymbol{x})\hat{\boldsymbol{u}} - u_c = R_2, \quad on\ \Gamma_u\,. \tag{7}$$

$$T(\boldsymbol{N}(\boldsymbol{x})\hat{\boldsymbol{u}}) - t = R_3, \quad on\ \Gamma_t\,. \tag{8}$$

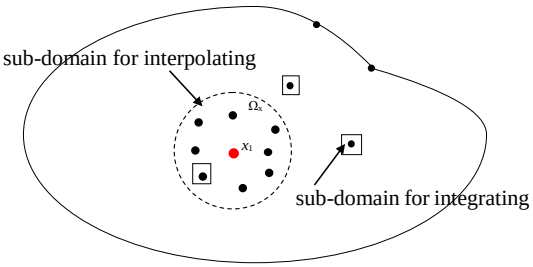

Fig. 2 Sub-domain for integration Ω_i and that for interpolation Ω_x

Then, we may use the method of weighted residuals for R_1, R_2 and R_3 with the nonconforming sub-domains, assuming K_d, K_s, and K_n to be the number of the nonconforming sub-domains for integration Ω_i, that of the collocation points on Γ_u, and that of the collocation points on Γ_t, respectively. Then, nonconforming sub-domains for integration Ω_i of number K_d may be selected in Ω, which are of simple configuration, for example a square for the 2D problems or a hexahedron for the 3D problems.

The weight functions for R_1 can be chosen as 1 in each sub-domain Ω_i and 0 otherwise. The collocation points x_j of number K_s and x_l of number K_n are selected on Γ_u and Γ_t, respectively. The weight functions for R_2 and R_3 may be chosen as the Dirac delta function. Then, the following equations are obtained:

$$\int_{\Omega_i}[D(\boldsymbol{N}(\boldsymbol{x})\hat{\boldsymbol{u}}) - b]\,d\Omega = 0, \quad i = 1, 2, \cdots, K_d\,. \tag{9}$$

$$[\boldsymbol{N}(\boldsymbol{x})\hat{\boldsymbol{u}} - u_c]_{x=x_j} = 0, \quad j = 1, 2, \cdots, K_s\,. \tag{10}$$

$$[T(\boldsymbol{N}(\boldsymbol{x})\hat{\boldsymbol{u}}) - t]_{x=x_l} = 0, \quad l = 1, 2, \cdots, K_n\,. \tag{11}$$

If we assume Ω_i to be simple-shaped and nonconforming, the integration on Ω_i may be very easy. On the other hand, as shown in (10) and (11), the collocation approach is applied to Γ_u and Γ_t to overcome a difficulty of selecting a simple-shaped sub-domain at boundary points of the domain Ω with complex shape. Also, some over-range collocation points are introduced so that the positivity conditions are satisfied for x_j and x_l.

Let us assume that the number of over-range points is K_o, then the number of unknown variables is $K_d + K_s + K_n + K_o$ for a scalar problem. To have the same number of the equations with that of the unknown variables, we use the following equations at x_j and x_l:

$$[D(\boldsymbol{N}(\boldsymbol{x})\hat{\boldsymbol{u}}) - b]_{x=x_j} = 0, \quad j = 1, 2, \cdots, K_s\,. \tag{12}$$

$$[D(\boldsymbol{N}(\boldsymbol{x})\hat{\boldsymbol{u}}) - b]_{x=x_l} = 0, \quad l = 1, 2, \cdots, K_n\,. \tag{13}$$

Equations (9)-(13) are the governing equations of the present SDMM. Because the number of equations of the SDMM is $K_d + 2(K_e + K_n)$ for the scalar problem, we obtain that the number of the over-range points K_o must be equal to the number of boundary points $K_e + K_n$. It is noted that the over-range points are used only for the interpolation at boundary points and neither satisfaction of any governing equation nor that of boundary condition is needed there.

The interpolation calculations are performed using the modified weighted least-square (MWLS) [10], in which the essential node condition can be imposed, at each sub-domain for interpolation Ω_x. The integration calculations of (9) are performed at each sub-domain for integration Ω_i. The calculations of (10) to (13) are performed using the ORCM.

In the ORCM, some over-range points are introduced which are located at outside of Ω. At the over-range points, no satisfaction of any governing partial differential equation or boundary condition is needed, so that the over-range points are not used in physics sense. While the over-range points can be used in interpolating calculation for points x_j and x_i, which is performed using the MWLS at Ω_x of points x_j or x_i.

III. Numerical Implementation

A. Error Estimation

For the purpose of error estimation and convergence studies, the Sobolev norm $\|u\|_0$ of function *u* is calculated. The norm for 2D problems is defined as:

$$\|u\|_0 = \left(\int_\Omega u^2 d\Omega\right)^{1/2}. \tag{14}$$

In addition, the Sobolev norm $\|\boldsymbol{q}\|_0$ of the first-order derivative vector of *u* for 2D problems is defined as:

$$\|\boldsymbol{q}\|_0 = \left(\int_\Omega \boldsymbol{q}^T \cdot \boldsymbol{q} d\Omega\right)^{1/2}. \tag{15}$$

With

$$\boldsymbol{q} = \left[\frac{\partial u}{\partial x} \quad \frac{\partial u}{\partial y}\right]^T = [q_x \quad q_y]^T. \tag{16}$$

and $\|\boldsymbol{q}\|_0$ is also calculated for the purpose of error estimation and convergence studies.

The relative errors for $\|u\|_0$ and $\|\boldsymbol{q}\|_0$ are, respectively, defined as:

$$R_0 = \frac{\|u^{num} - u^{exa}\|_0}{\|u^{exa}\|_0}. \tag{17}$$

$$R_q = \frac{\|q^{num} - q^{exa}\|_0}{\|q^{exa}\|_0}. \tag{18}$$

where u^{num} and $\boldsymbol{q}^{num}$ are numerical solutions, respectively, and u^{exa} and $\boldsymbol{q}^{exa}$ are the exact solutions, respectively.

B. Models of Calculation

Numerical solutions of a 2D nonlinear equation

$$\nabla^2 u + \varepsilon u^2 = e^x + 4e^{2y} + \varepsilon(e^{2x} + 2e^x e^{2y} + e^{4y}). \tag{19}$$

are obtained over a 0.3×0.1 domain of (0, 0)×(0.3, 0.1) (see Fig. 3) by using the SDMM and the CM. Substituting (19) into (9), we have the following equation:

Fig. 3 The object of calculation.

$$\left\{\int_{\Omega_i} \nabla^2(\boldsymbol{N}(\boldsymbol{x}))d\Omega\right\}\hat{\boldsymbol{u}} + \varepsilon\int_{\Omega_i}(\boldsymbol{N}(\boldsymbol{x})\hat{\boldsymbol{u}})^2 d\Omega = \int_{\Omega_i}(e^x + 4e^{2y})d\Omega + \varepsilon\int_{\Omega_i}(e^{2x} + 2e^x e^{2y} + e^{4y})d\Omega, \quad i = 1, 2, \cdots, K_d. \tag{20}$$

Because the quadratic basis is used in this paper, $\boldsymbol{N}(\boldsymbol{x})$ is a quadric function of $\boldsymbol{x}$, and $\nabla^2(\boldsymbol{N}(\boldsymbol{x}))$ is a constant vector. Ω_i is chosen as a square configuration in this paper, then, we have:

$$\int_{\Omega_i} \nabla^2(\boldsymbol{N}(\boldsymbol{x}))d\Omega = c^2\nabla^2(\boldsymbol{N}(\boldsymbol{x})). \tag{21}$$

where c^2 is the area of a square sub-domain Ω_i. The terms of the right-hand side of (20) can be calculated by analytically over Ω_i easily.

A mixed problem, the essential boundary condition is imposed at nodes on top and bottom boundaries and the natural boundary condition is prescribed at nodes on left and right boundaries, is solved. Regular (taking the same nodal interval *h*) nodal models of *h*=1/60 (197 nodes), *h*=1/80 (305 nodes) and *h*=1/100 (437 nodes) are, respectively, used to study the convergence with the nodal model refinement. Because ε in (19) is the coefficient of nonlinear term u^2 of (19), the value of ε affects the nonlinearity of the nonlinear problem, and the nonlinearity of the problem becomes strong as the value of ε becomes large. In order to solve the challenge issue of strong nonlinear problems, five kinds of ε which are $\varepsilon = 0.1$, $\varepsilon = 1$, $\varepsilon = 10$, $\varepsilon = 100$, and $\varepsilon = 200$ are used.

C. Results

The sub-domain of integration is chosen as a square configuration in this paper, and the area of the sub-domain of integration is c^2. To find optimal values of c, the problems with $\varepsilon = 0.1$ and $\varepsilon = 1$ are first calculated by using the SDMM. The results of relative errors R_0 and R_q are shown in Fig. 4 and Fig.5, respectively, where $c = kh$ and $0 < k < 2$. In the boxes of these figures, "*u*" means that the essential boundary condition is imposed at nodes on top and bottom boundaries,

and "q_x" means that the natural boundary condition is prescribed at nodes on left and right boundaries. For the regular nodal models, $k = 1$ means that the sub-domains of integration are conforming, $k < 1$ separated and $k > 1$ overlapped sub-domains, respectively. These figures show that the most accurate results are given at $k = 1.3$ for $\varepsilon = 0.1$ and $k = 0.8$ for $\varepsilon = 1$.

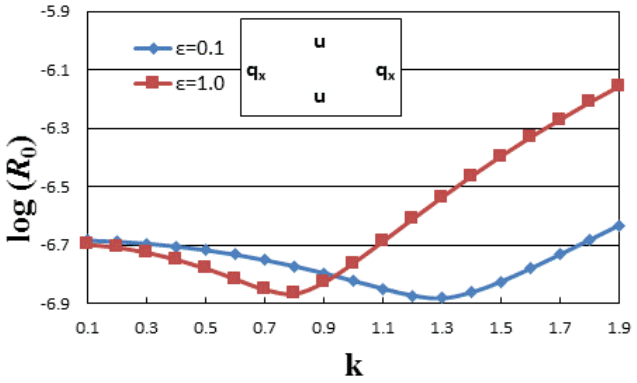

Fig. 4 Changes of relative error R_0 with k for $\varepsilon = 0.1$ and $\varepsilon = 1$.

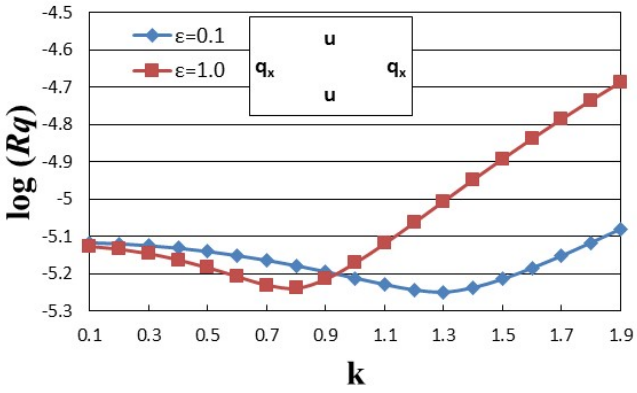

Fig. 5 Changes of relative error R_q with k for $\varepsilon = 0.1$ and $\varepsilon = 1$.

The relative errors R_0 and R_q for $\varepsilon = 0.1$ by using the SDMM and the CM are shown in Figs. 6 and 7, respectively. The relative errors R_0 and R_q for $\varepsilon = 1$ by using the SDMM and the CM are shown in Figs. 8 and 9, respectively. These figures show that the relative errors by using the SDMM are smaller than those by using the CM, and the relative errors of become smaller with the decrease of the nodal interval *h*.

The relative errors R_0 and R_q for all the values of ε by using the SDMM with $k = 1.3$ are shown in Figs. 10 and 11, respectively. It can be seen from these figures that although the error levels become higher with the increase of ε in general, the error levels using $\varepsilon = 0.1$, $\varepsilon = 1$ and $\varepsilon = 10$ are rather low, those using $\varepsilon = 100$ and $\varepsilon = 200$ are also lower, and the relative errors using all the values of ε become smaller with the decrease of the nodal interval *h*.

Finally, an irregular nodal model of 437 nodes is tested for $\varepsilon = 0.1$ and $\varepsilon = 1$. In these calculations, value of c=1/100, which is the same as the value of c used in the regular nodal model of 437 nodes, is used in the irregular nodal model. While for the irregular nodal model, it means that Ω_i are

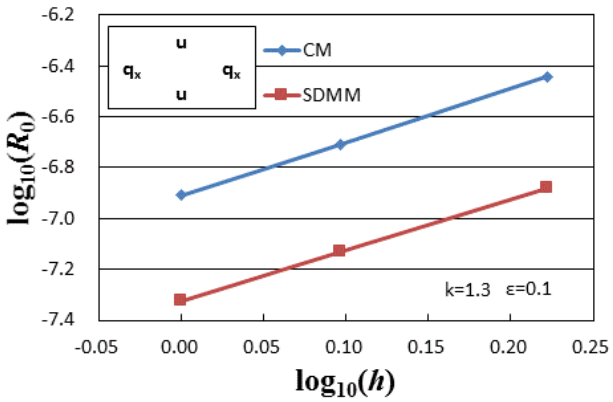

Fig. 6 The relative error R_0 with h for $\varepsilon = 0.1$.

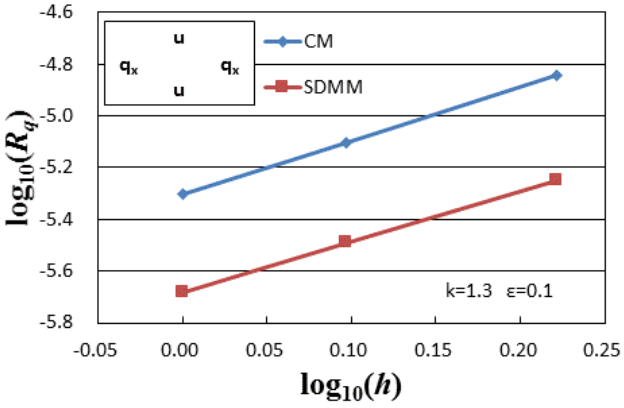

Fig. 7 The relative error R_q with h for $\varepsilon = 0.1$.

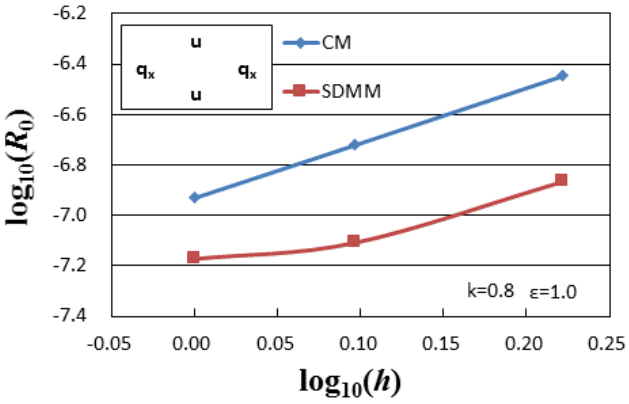

Fig. 8 The relative error R_0 with h for $\varepsilon = 1$.

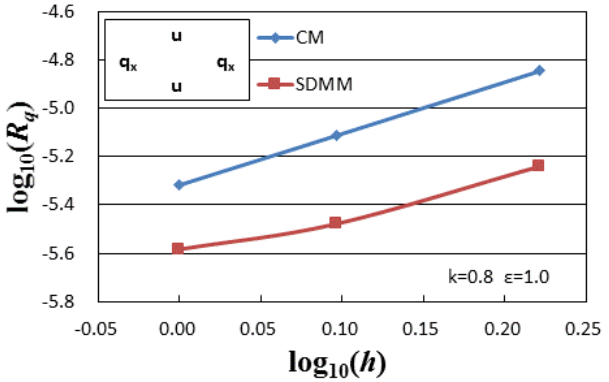

Fig. 9 The relative error R_q with h for $\varepsilon = 1$.

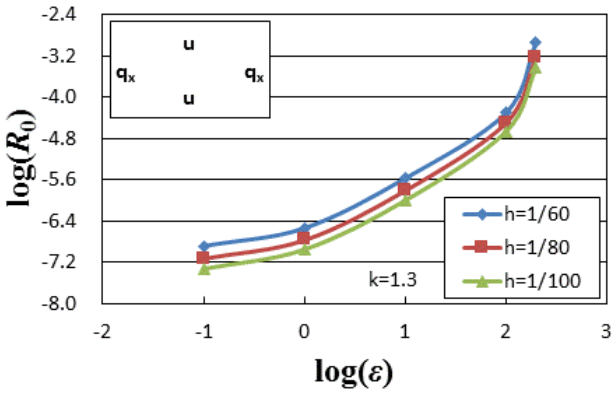

Fig. 10 The relative error R_0 using all the values of ε.

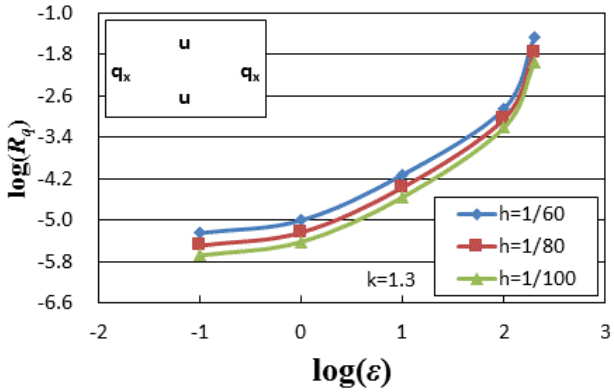

Fig. 11 The relative error R_q using all the values of ε.

nonconforming. The irregular nodal distribution of the nodes model is shown in Fig. 12.

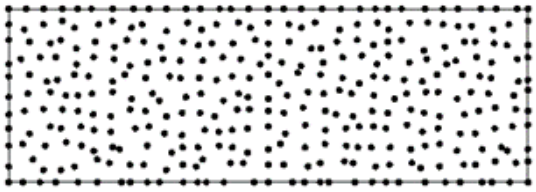

Fig. 12 The irregular nodal distributions (not including the over-range points) of 437 nodes model.

The distribution figure of *u* using regular node model (437 nodes) for $\varepsilon = 1$ is shown in Fig. 13, and the distribution figure of *u* using irregular node model (437 nodes) for $\varepsilon = 1$ is shown in Fig. 14. The distribution figure of the exact *u* is shown in Fig. 15. From these figures, it is seen that the present results by using the regular nodal model as well as the irregular nodal model are excellent.

IV. Conclusions

In the sub-domain meshless method (SDMM), which has been proposed by us, simple-shaped conforming or nonconforming sub-domains are used as for integration to make integration easy.

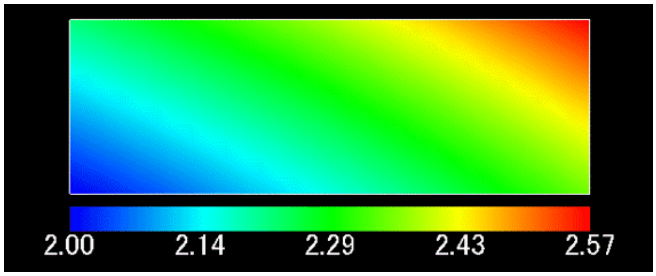

Fig. 13 The distribution figure of *u* using regular node model (437 nodes) for $\varepsilon = 1$.

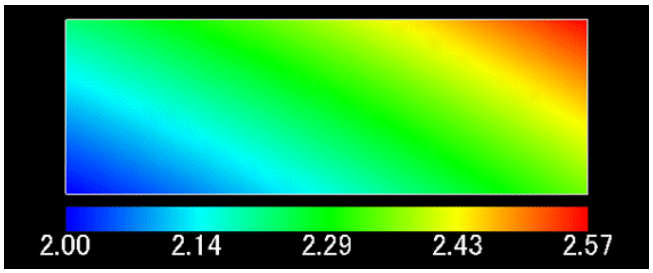

Fig. 14 The distribution figure of *u* using irregular node model (437 nodes) for $\varepsilon = 1$.

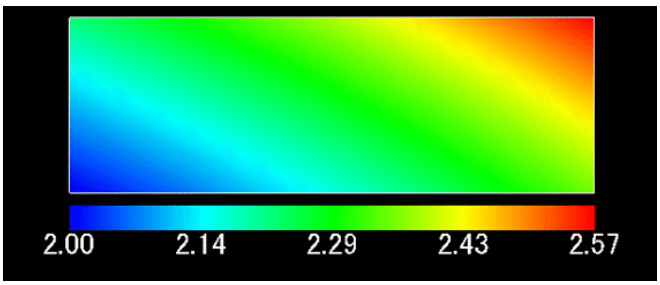

Fig. 15 The distribution figure of the exact *u*.

As is well known, nonlinear problems, especially strong nonlinear problems are difficult problems of the computational mechanics. Therefore, a nonlinear problem should be used for checking the accuracy and performance of the SDMM. In this paper, the nonlinear mixed boundary value problem is analyzed with some regular nodal models by using the SDMM and the CM, respectively, and it is seen that former gives more accurate results than the latter. It is also shown that the SDMM possesses not only good accuracy but excellent convergence characteristics for both the unknown variables and their derivatives for the above boundary value problem.

According to the tests on the nonlinear problem with the irregular nodal model, it is shown that the solutions by the SDMM are in good agreement with the exact solutions.

References

[1] J. S. Chen, C. T. Wu, S. Yoon, and Y. You, "A stabilized conforming nodal integration for Galerkin mesh-free methods," *Int. J. Numer. Methods Eng.*, vol. 50, 2001, pp. 435-466.

[2] J. S. Chen, M. Hillman, and M. Rüter, "An arbitrary order variationally consistent integration method for Galerkin meshfree methods," *Int. J. Numer. Methods Eng.*, vol. 95, 2013, pp. 387-418.

[3] S, V, Patanakar, *Numerical Heat Transfer and Fluid Flow*, Hemisphere, 1980.

[4] L. Demkowicz, A. Karafilt, and T. Liszka, "On some convergence results for FDM with irregular mesh," *Comput. Methods Appl. Mech. Eng.*, vol. 42 1984, pp. 343-355.
[5] X. Jin, G. Li, and N. R. Aluru, "Positivity conditions in meshless collocation methods," *Comput. Methods Appl. Mech. Eng.*, vol. 193, 2004, pp. 1171-1202.
[6] Y.-M., Guo, "An overrange collocation method," *Comput. Modeling Eng. Sci.*, vol. 73, 2011, pp. 1-22.
[7] Y.-M. Guo, H. Osako, and S. Kamitani, "Nonlinear analyses by using the ORCM," *J. Comput. Sci. Tech.*, vol. 7, 2013, pp. 114-125.
[8] Y.-M. Guo, K. Shioya, K. Oobuchi, G. Yagawa, and S. Kamitani, "Accuracy improvement of collocation method by using the over-range collocation points for 2-D and 3-D problems," *Mech. Eng. J.*, vol. 1, no. 2, 2014, pp. 1-19.
[9] Y.-M. Guo and G. Yagawa, "A meshless method with conforming and nonconforming sub-domains," *Int. J. Numer. Methods Eng.*, vol. 110: 2017, pp. 826-841.
[10] S. Rajendran and B. R. Zhang, "A "FE-meshfree" QUAD4 element based on partition of unity," *Comput. Methods Appl. Mech. Eng.*, vol. 197, 2007, pp. 128-147.